# Structure of the core oligosaccharide of a rough-type lipopolysaccharide of *Pseudomonas syringae* pv. *phaseolicola*

**Evelina L. Zdorovenko**[1,2], **Evgeny Vinogradov**[1,*], **Galina M. Zdorovenko**[3], **Buko Lindner**[2], **Olga V. Bystrova**[1,2], **Alexander S. Shashkov**[1], **Klaus Rudolph**[4], **Ulrich Zähringer**[2] and **Yuriy A. Knirel**[1,2]

[1]*N. D. Zelinsky Institute of Organic Chemistry, Russian Academy of Sciences Moscow, Russia;* [2]*Research Center Borstel, Leibniz Center for Medicine and Biosciences, Borstel, Germany;* [3]*D.K. Zabolotny Institute of Microbiology and Virology, National Academy of Sciences of Ukraine, Kiev, Ukraine;* [4]*Institute for Plant Pathology and Plant Defence, Georg August University, Göttingen, Germany*

The core structure of the lipopolysaccharide (LPS) isolated from a rough strain of the phytopathogenic bacterium *Pseudomonas syringae* pv. *phaseolicola*, GSPB 711, was investigated by sugar and methylation analyses, Fourier transform ion-cyclotron resonance ESI MS, and one- and two-dimensional $^1$H-, $^{13}$C- and $^{31}$P-NMR spectroscopy. Strong alkaline deacylation of the LPS resulted in two core-lipid A backbone undecasaccharide pentakisphosphates in the ratio $\approx$ 2.5 : 1, which corresponded to outer core glycoforms 1 and 2 terminated with either L-rhamnose or 3-deoxy-D-*manno*-oct-2-ulosonic acid (Kdo), respectively. Mild acid degradation of the LPS gave the major glycoform 1 core octasaccharide and a minor truncated glycoform 2 core heptasaccharide, which resulted from the cleavage of the terminal Kdo residues. The inner core of *P. syringae* is distinguished by a high degree of phosphorylation of L-*glycero*-D-*manno*-heptose residues with phosphate, diphosphate and ethanolamine diphosphate groups. The glycoform 1 core is structurally similar but not identical to one of the core glycoforms of the human pathogenic bacterium *Pseudomonas aeruginosa*. The outer core composition and structure may be useful as a chemotaxonomic marker for the *P. syringae* group of bacteria, whereas a more conserved inner core structure appears to be representative for the whole genus *Pseudomonas*.

*Keywords*: core oligosaccharide; glycoform; lipopolysaccharide structure; phytopathogen; *Pseudomonas syringae*.

The bacteria *Pseudomonas syringae* cause serious diseases in most cultivated plants and are widespread in nature as epiphytes. More than 50 pathovars of *P. syringae* and related species have been described based on the distinctive pathogenicity of the strains to one or more host plants [1]. The *P. syringae* group is characterized by a high degree of heterogeneity also in respect to genomic features. Recently, type strains of various *P. syringae* pathovars have been delineated into nine genomospecies [2]. However, the taxonomic status of the pathovars and genomospecies remains uncertain.

The lipopolysaccharide (LPS) is the major component of the outer membrane of Gram-negative bacteria, which plays an important role in interaction of bacteria with their hosts. LPS is composed of lipid A, a core oligosaccharide, and an O-polysaccharide (O-antigen) built up of oligosaccharide repeats. The structures of the O-polysaccharides of all known serologically distinguishable smooth strains of *P. syringae* have been determined [3–12]. Aiming at solving the problems of recognition, taxonomy and classification of *P. syringae* strains, we established, for the first time, the full structure of the core region of the LPS from a rough strain of *P. syringae* pv. *phaseolicola* GSPB 711. According to published composition [11,13–16] and serological [17,18] data, this core structure is shared by most *P. syringae* strains tested.

## Materials and methods

### Bacterium, growth and isolation of the lipopolysaccharide

*P. syringae* pv. *phaseolicola* rough strain GSPB 711 was received from the Göttingen Collection of Plant Pathogenic Bacteria (Germany) were grown on Potato agar at 22 °C for 24 h, washed with physiological saline, separated by centrifugation, washed with acetone and dried.

LPS was isolated from dry bacterial cells by the method of Galanos [19] and purified by ultracentrifugation (105 000 *g*, 4 h). The supernatant was dialyzed against distilled water and lyophilized.

## Alkaline degradation of the lipopolysaccharide

The LPS (110 mg) was treated with anhydrous hydrazine (4 mL) for 1 h at 37 °C, then 16 h at 20 °C. Hydrazine was flushed out in a stream of air at 30–33 °C, the residue washed with cold acetone at 4 °C, dried in vacuum, dissolved in 4 M NaOH (8 mL) supplemented with a small amount of NaBH$_4$, and then heated at 100 °C for 4 h. After cooling to 4 °C, the solution was acidified to pH 5.5 with concentrated HCl, extracted twice with dichloromethane, and the aqueous solution desalted by gel-permeation chromatography on a column (60 × 2.5 cm) of Sephadex G-50 (Amersham Biosciences, Uppsala, Sweden) in pyridinium acetate buffer (4 mL pyridine and 10 mL HOAc in 1 L water, pH 4.5) at 30 mL·h$^{-1}$. Elution was monitored with a differential refractometer (Knauer, Berlin, Germany). The isolated oligosaccharide mixture (OS$_{NaOH}$) (35 mg) was fractionated by high-performance anion-exchange chromatography (HPAEC) on a semipreparative CarboPac PA1 column (250 × 9 mm; Dionex, Sunnyvale, CA, USA) using a linear gradient of 0.02–0.6 M NaOAc in 0.1 M NaOH at a flow rate of 2 mL·min$^{-1}$ for 100 min and 2-mL fractions were collected and analyzed by HPAEC using pulsed amperometric detection (Dionex) on an analytical CarboPac PA1 column (250 × 4.6 mm) using the same eluent at 1 mL·min$^{-1}$ for 30 min. Desalting on a column (40 × 2.6 cm) of Sephadex G-50 afforded two major oligosaccharides, OS$_{NaOH}$-I and OS$_{NaOH}$-II (7.2 and 3.6 mg, respectively), having retention times 11.7 and 18.0 min in analytical HPAEC.

## Mild-acid degradation of the lipopolysaccharide

The LPS was dissolved in aqueous 1% HOAc and heated for 1.5 h at 100 °C. The precipitate was removed by centrifugation (12 000 *g*, 20 min), and the supernatant fractionated by gel-permeation chromatography on a column (40 × 2.6 cm) of Sephadex G-50 as described above to give a mixture of phosphorylated oligosaccharides (OS$_{HOAc}$).

## Chemical analysis

For neutral sugar analysis, the oligosaccharides (0.5 mg each) were hydrolyzed with 2 M CF$_3$CO$_2$H (120 °C, 2 h), monosaccharides were conventionally converted into the alditol acetates and analyzed by GLC on a Hewlett-Packard HP 5890 Series II chromatograph (Palo Alto, CA, USA) equipped with a 30-m fused-silica SPB-5 column (Supelco, Bellefoute, PA, USA) using a temperature gradient of 150 °C (3 min) → 320 °C at 5 °C·min$^{-1}$. After hydrolysis of the oligosaccharides (40 µg each) with 4 M HCl (80 µL, 100 °C, 16 h), amino components were analyzed as phenylthiocarbamoyl derivatives by HPLC on a reversed-phase Pico-Tag column (150 × 3.9 mm) using buffers for Pico-Tag amino acid analysis of protein hydrolysates (Waters, Milford, MA, USA) at 42 °C and a flow rate 1 mL·min$^{-1}$ for 10 min; monitoring was performed with a dual λ absorbance detector (Waters) at 254 nm.

## Methylation analysis

OS$_{NaOH}$-I and OS$_{NaOH}$-II (1 mg each) were dephosphorylated with aqueous 48% HF (25 µL) at 4 °C for 16 h, the solution was diluted with water and lyophilized, the products were N-acetylated with Ac$_2$O (100 µL) in aqueous saturated NaHCO$_3$ at 20 °C for 1 h at stirring, reduced with NaBH$_4$ and desalted by gel-permeation chromatography on Sephadex G-15. Methylation was performed by the procedure of Ciucanu and Kerek [20] with CH$_3$I (0.3 mL) in dimethylsulfoxide (0.5 mL) in the presence of solid NaOH (stirring for 20 min before and 2 h after adding CH$_3$I), the reaction mixture was diluted with water, the methylated compounds were extracted with chloroform, hydrolyzed with 3 M CF$_3$CO$_2$H (100 °C, 2 h), reduced with NaBD$_4$, acetylated and analyzed by GLC MS on a HP Ultra 1 column (25 m × 0.3 mm) using a Varian Saturn 2000 instrument (Palo Alto, CA, USA) equipped with an ion-trap MS detector.

## Electrospray ionization mass spectrometry (ESI MS)

High-resolution electrospray ionization Fourier transform ion-cyclotron resonance mass spectrometry (ESI FT-ICR MS) was performed in the negative ion mode using an ApexII-instrument (Bruker Daltonics, Billerica, USA) equipped with a 7 T actively shielded magnet and an Apollo electrospray ion source. Mass spectra were acquired using standard experimental sequences as provided by the manufacturer. Samples were dissolved at a concentration of ≈ 10 ng·µL$^{-1}$ in a 50 : 50 : 0.001 (v/v/v) 2-propanol, water, and triethylamine mixture and sprayed at a flow rate of 2 µL·min$^{-1}$. Capillary entrance voltage was set to 3.8 kV, and dry gas temperature to 150 °C. Capillary skimmer dissociation (CSD) was induced by increasing the capillary exit voltage from −100 to −350 V.

## NMR spectroscopy

NMR spectra were obtained on a Varian Inova 500, Bruker DRX-500 and DRX-600 spectrometers (Karlsruhe, Germany) in 99.96% D$_2$O at 25 or 50 °C and pD 3, 6 or 9 (uncorrected), respectively, using internal acetone (δ$_H$ 2.225, δ$_C$ 31.45) or external aqueous 85% H$_3$PO$_4$ (δ$_P$ 0.0) as reference. Prior to the measurements, the samples were lyophilized twice from D$_2$O. Bruker software XWINNMR 2.6 was used to acquire and process the data. Mixing times of 120 and 100 ms were used in TOCSY and 250 and 225 ms in ROESY experiments at 500 and 600 MHz, respectively.

## Results and Discussion

Oligosaccharides derived by strong alkaline degaradation of the LPS [21] were used to determine the structure of the core-lipid A carbohydrate backbone of the *P. syringae* LPS. The LPS was O-deacetylated by mild hydrazinolysis and then N-deacylated under strong alkaline conditions (4 M NaOH, 100 °C, 4 h). After desalting, the resultant mixture of oligosaccharides (OS$_{NaOH}$) was fractionated by HPAEC on CarboPak PA1 at super-high pH to give the major and minor products (OS$_{NaOH}$-I and OS$_{NaOH}$-II, respectively).

The charge deconvoluted ESI FT-ICR mass spectrum of OS$_{NaOH}$ showed an abundant molecular ion with the molecular mass 2356.55 Da as well as less intense peaks (Fig. 1). The measured molecular masses of two ions, 2356.55 and 2430.57 Da, were in agreement with those
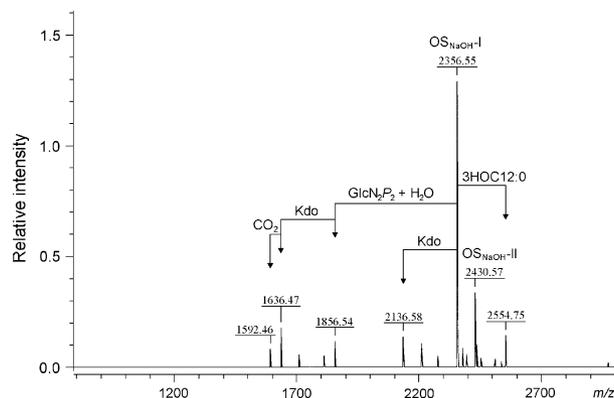
**Fig. 1. Charge deconvoluted negative ion ESI FT-ICR mass spectrum of OS$_{NaOH}$ obtained by strong alkaline degradation of the LPS.** 3HOC12:0 stands for the 3-hydroxydodecanoyl group.

calculated for undecasaccharide pentakisphosphates having the following composition: 6dHex$_1$Hex$_2$Hep$_2$Kdo$_2$HexN$_4P_5$ and Hex$_2$Hep$_2$Kdo$_3$HexN$_4P_5$ (OS$_{NaOH}$-I and OS$_{NaOH}$-II, respectively), where 6dHex stands for a 6-deoxyhexose, Hex for a hexose, Hep for a heptose, HexN for a hexosamine, and Kdo for 3-deoxy-D-*manno*-oct-2-ulosonic acid. These compounds differ in one of the constituent monosaccharides, which is either a 6dHex residue or the third Kdo residue. Accordingly, the $^1$H-NMR spectra of OS$_{NaOH}$-I and OS$_{NaOH}$-II isolated by HPAEC showed signals for two and three Kdo residues, respectively. This finding is in agreement with a significantly higher retention time of OS$_{NaOH}$-II in HPAEC as compared with OS$_{NaOH}$-I due to the presence of an additional negatively charged Kdo residue.

As depicted in Fig. 1, the other minor mass peaks belonged to (a) OS$_{NaOH}$-I bearing a 3-hydroxydodecanoyl group ($\Delta m/z$ 198), which resulted from incomplete N-deacylation of lipid A, and (b) to fragment ions due to losses of Kdo ($\Delta m/z$ −220), bisphosphorylated diglucosamine lipid A backbone ($\Delta m/z$ −500), and decarboxylation ($\Delta m/z$ −44).

The $^1$H- and $^{13}$C-NMR spectra of OS$_{NaOH}$-I and OS$_{NaOH}$-II at two different temperature and pD conditions were assigned using two-dimensional COSY, TOCSY and $^1$H,$^{13}$C HSQC experiments (Table 1). Spin systems for all constituent monosaccharides, including rhamnose (Rha), Glc, L-*glycero*-D-*manno*-heptose (Hep), GlcN, GalN and Kdo, were identified by $^3J$ coupling constants and using published data for structurally similar oligosaccharides derived from the *Pseudomonas aeruginosa* LPS [22,23]. The configurations of the glycosidic linkages were determined based on $J_{1,2}$ coupling constant values for Glc, GlcN and GalN (3–3.5 and 7–8 Hz for α- and β-linked monosaccharides, respectively) and by typical $^1$H- and $^{13}$C-NMR chemical shifts for Rha, Hep and Kdo [24]. The anomeric configurations of Rha and Hep were confirmed by the presence of H-1,H-2 and no H-1,H-3 or H-1,H-5 cross-peaks in the two-dimensional ROESY spectra of the oligosaccharides.

Linkage and sequence analysis of OS$_{NaOH}$-I and OS$_{NaOH}$-II was performed using a two-dimensional ROESY experiment. This revealed a lipid A carbohydrate backbone of a GlcN$^{II}$→GlcN$^I$ disaccharide and an inner core region composed of two Hep and two Kdo residues (Hep$^I$, Hep$^{II}$, Kdo$^I$ and Kdo$^{II}$). The ROESY correlation pattern was essentially identical to that reported earlier for the inner core of the other *Pseudomonas* LPS studied [22,23,25]. In particular, a correlation of Kdo$^{II}$ H6 with Kdo$^I$ H3eq at δ 3.98/2.26 showed the presence of an α2→4-linkage between these residues, and a correlation of Hep$^I$ H1 with Kdo$^I$ H5 and H7 at δ 5.39/4.27 and 5.39/3.87, respectively, is characteristic for an α1→5-linkage [25].

The following correlations in the ROESY spectrum of OS$_{NaOH}$-I were observed between the anomeric protons of the outer core monosaccharides and the protons at the linkage carbons of the neighboring monosaccharide residues: GalN H1/Hep$^I$ H3 at δ 5.50/4.09; Glc$^I$ H1/GalN H3 at δ 4.69/4.25; Glc$^{II}$ H1/GalN H4 at δ 4.97/4.35; GlcN$^{III}$ H1/Glc$^I$ H2 at δ 4.57/3.31; Rha H1/Glc$^{II}$ H6a,6b at δ 4.77/3.79 and 4.77/3.91. These data were in agreement with methylation analysis data (see below) and $^{13}$C-NMR chemical shift data showing downfield displacements of the signals for the corresponding linkage carbons (Table 2) as compared with their positions in the nonsubstituted monosaccharides [26].

In the $^{31}$P-NMR spectrum of OS$_{NaOH}$-I, five signals for phosphate groups were present at δ 2.58, 2.72, 4.29, 4.47 and 4.95 (at pD 6). A two-dimensional $^1$H,$^{31}$P-HMQC experiment with OS$_{NaOH}$-I revealed a pattern essentially identical to that of *Pseudomonas aeruginosa* core-lipid A backbone oligosaccharide pentakisphosphate [22,23] and defined the positions of the phosphate groups at GlcN$^I$ O1, GlcN$^{II}$ O4, Hep$^I$ O2 and O4 and Hep$^{II}$ O6. These data together demonstrated that OS$_{NaOH}$-I has the structure shown in Fig. 2.

Similar studies, including ROESY and $^1$H,$^{31}$P-HMQC experiments, demonstrated that OS$_{NaOH}$-II has the same structure except for that the terminal Rha residue in the outer core region is replaced with a terminal Kdo residue (Kdo$^{III}$). The chemical shift for H3eq in Kdo$^{III}$ was similar to that in α-Kdo$^{II}$ and published values for α-linked Kdo [27] (δ 2.17 vs. 2.06–2.13) and significantly different from published data for β-linked Kdo [27] (δ 2.37–2.47), thus indicating the α-configuration of Kdo$^{III}$.

An additional $^1$H,$^{13}$C-HMBC experiment confirmed the linkage pattern and the sugar sequence in OS$_{NaOH}$-II but failed to reveal correlation for Kdo$^{III}$ C2 to a proton at the linkage carbon of the neighbouring sugar. Substitution with a keto sugar is known to cause a small downfield displacement of the linkage carbon signal (α-effect of glycosylation), and no displacement was observed in the $^{13}$C-NMR spectrum of OS$_{NaOH}$-II for the C6 signal of Glc$^{II}$, which is a putative linkage carbon for Kdo$^{III}$ (Table 2). However, the attachment of Kdo$^{III}$ at position 6 of Glc$^{II}$ could be demonstrated by a significant upfield β-effect of glycosylation on the C5 signal from δ 73.2 in nonsubstituted α-Glc [26] to δ 71.9 in Glc$^{II}$ as well as by displacements of the H4-H6 signals from δ 3.42, 3.84, 3.84, respectively, in nonsubstituted Glc [28] to δ 3.66, 4.03, 3.43, respectively, in Glc$^{II}$ as a result of the anisotropy of the carboxyl carbon of Kdo$^{III}$. The data obtained suggested that OS$_{NaOH}$-II has the structure shown in Fig. 2.

The structures of the alkaline degradation products were further confirmed by methylation analysis after dephosphorylaton, N-acetylation and borohydride reduction. The

**Table 1. 500-Mz ¹H-NMR chemical shifts at pD 6 at 25 °C (δ).**

| Compound | Unit | | | | | | | |
|---|---|---|---|---|---|---|---|---|
| | H1<br>H3ax | H2<br>H3eq | H3<br>H4 | H4<br>H5 | H5<br>H6 | H6a<br>H7 | H6b<br>H8a | (7a) H7b<br>H8b |
| OS$_{NaOH}$-I | 5.48 | 2.99 | 3.72 | 3.47 | 4.09 | 3.74 | 4.28 | |
| →-6)-α-GlcN$^I$-(1→$P$[a] | 5.48 | 2.99 | 3.72 | 3.47 | 4.09 | 3.74 | 4.28 | |
| →6)-α-GlcN$^I$-(1→$P$ | 5.76 | 3.48 | 3.94 | 3.64 | 4.14 | 3.82 | 4.28 | |
| →6)-β-GlcN$^{II}$4$P$-(1→[a] | 4.59 | 2.82 | 3.65 | 3.65 | 3.65 | 3.42 | 3.67 | |
| →6)-β-GlcN$^{II}$4$P$-(1→ | 4.87 | 3.16 | 3.91 | 3.87 | 3.78 | 3.53 | 3.77 | |
| →4,5)-α-Kdo$^I$-(2→[a] | 1.96 | 2.26 | 4.17 | 4.24 | 3.68 | 3.87 | 3.61 | 3.89 |
| →4,5)-α-Kdo$^I$-(2→ | 2.08 | 2.27 | 4.16 | 4.32 | 3.75 | 3.87 | 3.61 | 3.90 |
| α-Kdo$^{II}$-(2→[a] | 1.77 | 2.04 | 4.28 | 4.07 | 3.63 | 3.98 | 3.64 | 3.92 |
| α-Kdo$^{II}$-(2→ | 1.87 | 2.12 | 4.17 | 4.10 | 3.67 | 3.98 | 3.69 | 4.01 |
| →3)-α-Hep$^I$2$P$4$P$-(1→[a] | 5.39 | 4.38 | 4.09 | 4.33 | 4.32 | 4.15 | 3.81 | 4.00 |
| →3)-α-Hep$^I$2$P$4$P$-(1→ | 5.37 | 4.55 | 4.21 | 4.52 | 4.28 | 4.12 | 3.81 | 3.96 |
| →3)-α-Hep$^{II}$6$P$-(1→[a] | 5.21 | 4.32 | 4.15 | 4.21 | 3.94 | 4.39 | 3.71 | 3.71 |
| →3)-α-Hep$^{II}$6$P$-(1→ | 5.15 | 4.41 | 4.21 | 4.12 | 4.05 | 4.55 | 3.75 | 3.81 |
| →3,4)-α-GalN-(1→[a] | 5.50 | 3.62 | 4.25 | 4.35 | 4.23 | 3.79 | 3.86 | |
| →3,4)-α-GalN-(1→ | 5.60 | 3.87 | 4.43 | 4.47 | 4.25 | 3.83 | 3.91 | |
| →2)-β-Glc$^I$-(1→[a] | 4.69 | 3.31 | 3.74 | 3.35 | 3.48 | 3.69 | 3.92 | |
| →2)-β-Glc$^I$-(1→ | 4.75 | 3.37 | 3.76 | 3.40 | 3.49 | 3.73 | 3.96 | |
| →6)-α-Glc$^{II}$-(1→[a] | 4.97 | 3.49 | 3.73 | 3.61 | 4.24 | 3.79 | 3.91 | |
| →6)-α-Glc$^{II}$-(1→ | 5.03 | 3.54 | 3.75 | 3.67 | 4.22 | 3.81 | 3.95 | |
| β-GlcN$^{III}$-(1→[a] | 4.57 | 2.77 | 3.36 | 3.49 | 3.42 | 3.82 | 3.88 | |
| β-GlcN$^{III}$-(1→ | 4.96 | 3.26 | 3.72 | 3.60 | 3.57 | 3.89 | 3.92 | |
| α-L-Rha-(1→[a] | 4.77 | 3.99 | 3.78 | 3.42 | 3.73 | 1.28 | | |
| α-L-Rha-(1→ | 4.80 | 4.02 | 3.82 | 3.44 | 3.76 | 1.32 | | |
| | | | | | | | | |
| OS$_{NaOH}$-II | 5.77 | 3.50 | 3.94 | 3.65 | 4.14 | 3.83 | 4.31 | |
| →-6)-α-GlcN$^I$-(1→$P$ | 5.77 | 3.50 | 3.94 | 3.65 | 4.14 | 3.83 | 4.31 | |
| →6)-β-GlcN$^{II}$4$P$-(1→ | 4.86 | 3.16 | 3.91 | 3.87 | 3.78 | 3.51 | 3.76 | |
| →4,5)-α-Kdo$^I$-(2→ | 2.07 | 2.28 | 4.15 | 4.32 | 3.74 | 3.88 | 3.61 | 3.92 |
| α-Kdo$^{II}$-(2→ | 1.86 | 2.12 | 4.18 | 4.10 | 3.68 | 4.03 | 3.70 | 4.00 |
| →3)-α-Hep$^I$2$P$4$P$-(1→ | 5.39 | 4.56 | 4.21 | 4.53 | 4.33 | 4.13 | 3.83 | 4.00 |
| →3)-α-Hep$^{II}$6$P$-(1→ | 5.15 | 4.41 | 4.22 | 4.12 | 4.05 | 4.56 | 3.76 | 3.83 |
| →3,4)-α-GalN-(1→ | 5.60 | 3.79 | 4.36 | 4.47 | 4.24 | 3.90 | 3.93 | |
| →2)-β-Glc$^I$-(1→ | 4.71 | 3.57 | 3.66 | 3.53 | 3.46 | 3.78 | 3.94 | |
| →6)-α-Glc$^{II}$-(1→ | 5.06 | 3.54 | 3.73 | 3.66 | 4.03 | 3.43 | 3.75 | |
| β-GlcN$^{III}$-(1→ | 5.01 | 3.25 | 3.79 | 3.56 | 3.52 | 3.86 | 3.86 | |
| α-Kdo$^{III}$-(1→ | 1.82 | 2.17 | 4.12 | 4.06 | 3.62 | 3.96 | 3.64 | 3.94 |

[a] Data at pD 9 at 50 °C.

analysis of OS$_{NaOH}$-I revealed terminal Rha, 2-substituted and 6-substituted Glc, 3-substituted Hep, 6-substituted 2-acetamido-2-deoxyglucitol (GlcNAc-ol; from GlcN-$P$ of lipid A), terminal GlcNAc and 3,4-disubstituted GalNAc in the ratios 0.67 : 1 : 1.67 : 0.5 : 0.83 : 0.75 : 0.17 (detector response), respectively, as well as a trace amount of terminal Glc. No 6-substituted GlcNAc, expected from GlcN4$P$ of lipid A was observed, most likely, owing to cleavage of the Kdo residue attached to GlcN4$P$ at position 6 in the course of dephosphorylaton of OS$_{NaOH}$-I under acidic conditions that converted the 6-substituted residue into a terminal residue. A similar analysis of OS$_{NaOH}$-II resulted in identification of terminal, 2-substituted and 6-substituted Glc, 3-substituted Hep, 6-substituted GlcNAc-ol, terminal GlcNAc and 3,4-disubstituted GalNAc in the ratios 1.25 : 1 : 1.25 : 0.38 : 1.13 : 0.63 : 0.13, respectively, as well as a trace amount of terminal Rha. These data could be accounted for by the attachment of Kdo$^{III}$ in OS$_{NaOH}$-II to

the same position 6 of one of the Glc residues as Rha in OS$_{NaOH}$-I, whereas terminal Glc resulted from partial removal of Kdo$^{III}$ from 6-substituted Glc during dephosphorylation of OS$_{NaOH}$-II.

For analysis of alkali-labile groups, the LPS was subjected to mild-acid hydrolysis and an oligosaccharide mixture (OS$_{HOAc}$) was isolated by gel-permeation chromatography on Sephadex G-50. Sugar analysis of OS$_{HOAc}$ by GLC of the acetylated alditols revealed Rha, Glc, Hep, GlcN and GalN in the ratios 1 : 2.5 : 0.7 : 0.5 : 0.1 (detector response), respectively, and analysis using an amino acid analyser showed the presence of alanine and ethanolamine.

Charge deconvoluted negative ion ESI FT-ICR mass-spectrum of OS$_{HOAc}$ (not shown) displayed a number of molecular ions, the most abundant from which had the molecular masses 1810.53 and 1933.52 Da and could be assigned to a Rha$_1$Glc$_2$Hep$_2$Kdo$_1$HexN$_2$$P_3$Ac$_1$Ala$_1$Cm$_1$ octasaccharide trisphosphate (OS$_{HOAc}$-I) and that contain-

**Table 2. 125-MHz $^{13}$C-NMR chemical shifts at pD 6 at 25 °C (δ).**

| Compound | Unit C1 | C2 | C3 | C4 | C5 | C6 | C7 | C8 |
|---|---|---|---|---|---|---|---|---|
| OS$_{NaOH}$-I | | | | | | | | |
| →-6)-α-GlcN$^I$1$P$ | 93.9 | 56.1 | 72.9 | 71.0 | 73.0 | 70.7 | | |
| →6)-β-GlcN$^{II}$4$P$-(1→ | 102.4 | 57.0 | 74.3 | 75.4 | 75.4 | 63.9 | | |
| →4,5)-α-Kdo$^I$-(2→ | | 100.7 | 35.5 | 72.3 | 68.9 | 73.4 | 70.1 | 65.0 |
| α-Kdo$^{II}$-(2→ | | 102.8 | 36.3 | 66.6 | 67.9 | 73.3 | 72.0 | 64.0 |
| →3)-α-Hep$^I$2$P$4$P$-(1→ | 98.6 | 74.8 | 75.5 | 70.1 | 73.7 | 69.9 | 64.2 | |
| →3)-α-Hep$^{II}$6$P$-(1→ | 103.3 | 70.1 | 78.0 | 66.6 | 73.0 | 73.3 | 63.0 | |
| →3,4)-α-GalN-(1→ | 97.6 | 51.5 | 79.5 | 76.6 | 73.4 | 60.7 | | |
| →2)-β-Glc$^I$-(1→ | 104.6 | 84.1 | 76.7 | 71.1 | 76.5 | 61.9 | | |
| →6)-α-Glc$^{II}$-(1→ | 100.2 | 72.9 | 73.8 | 69.8 | 71.4 | 67.3 | | |
| β-GlcN$^{III}$-(1→ | 106.0 | 58.3 | 76.7 | 70.3 | 77.0 | 61.5 | | |
| α-L-Rha-(1→ | 102.1 | 71.0 | 71.2 | 73.1 | 69.6 | 18.0 | | |
| | | | | | | | | |
| OS$_{NaOH}$-II | | | | | | | | |
| →-6)-α-GlcN$^I$1$P$ | 93.4 | 55.8 | 70.9 | 71.2 | 72.3 | 71.1 | | |
| →6)-β-GlcN$^{II}$4$P$-(1→ | 100.7 | 57.3 | 73.3 | 76.1 | 75.5 | 64.2 | | |
| →4,5)-α-Kdo$^I$-(2→ | | | 35.9 | 72.8 | 69.7 | 73.9 | 70.7 | 65.4 |
| α-Kdo$^{II}$-(2→ | | | 36.6 | 67.3 | 68.2 | 74.2 | 72.3 | 64.8 |
| →3)-α-Hep$^I$2$P$4$P$-(1→ | 98.9 | 76.1 | 75.7 | 72.2 | 73.7 | 70.8 | 64.8 | |
| →3)-α-Hep$^{II}$6$P$-(1→ | 103.8 | 70.9 | 79.8 | 67.1 | 73.3 | 74.9 | 63.1 | |
| →3,4)-α-GalN-(1→ | a | 52.4 | 79.0 | 80.8 | 73.4 | 61.9 | | |
| →2)-β-Glc$^I$-(1→ | 104.8 | 85.5 | 77.4 | 71.4 | 77.7 | 62.8 | | |
| →6)-α-Glc$^{II}$-(1→ | 102.7 | 73.5 | 74.9 | 70.4 | 71.9 | 61.9 | | |
| β-GlcN$^{III}$-(1→ | 106.0 | 58.3 | 76.7 | 70.3 | 77.0 | 61.5 | | |
| α-Kdo$^{III}$-(1→ | | 101.1 | 35.8 | 67.8 | 67.7 | 73.1 | 71.1 | 65.1 |

[a] No H1,C1 cross-peak was present in the $^1$H,$^{13}$C HSQC spectrum.

ing an additional ethanolamine phosphate group (Etn$P$) (OS$_{HOAc}$-II). Two other nonsugar groups present in OS$_{HOAc}$, *viz.* N-alanyl and O-carbamoyl (Cm) groups, are conserved components of the LPS core of pseudomonads [29–31]; Ala is typically linked to GalN, and the location of Cm at Hep$^{II}$ O7 in the LPS of *P. syringae* has been demonstrated earlier [32].

Further mass peaks belonged to the oligosaccharides that contain one phosphate group more than OS$_{HOAc}$-I and OS$_{HOAc}$-II ($\Delta m/z$ 80) and, hence, include a diphosphate group. Another series of less intense mass peaks corresponded to Rha-lacking heptasaccharides with molecular masses 1664.43 and 1787.47 Da (OS$_{HOAc}$-III and OS$_{HOAc}$-IV, respectively). They were evidently derived from the corresponding octasaccharides that initially contained Kdo$^{III}$, which was cleaved by mild-acid hydrolysis. Yet another minor series belonged to GlcNAc-lacking compounds ($\Delta m/z$ −203), and, finally, each ion was accompanied by an ion with Kdo$^I$ in an anhydro form ($\Delta m/z$ −18) [33].

The CSD negative ion ESI FT-ICR mass spectrum of OS$_{HOAc}$ (Fig. 3) showed a cleavage of the glycosidic linkage between Hep$^I$ and Hep$^{II}$ accompanied by a partial loss of the carbamoyl group ($\Delta m/z$ −43) [22–24]. The major Z-fragments from the reducing end with $m/z$ 571.10, 651.08 and 694.13 contained Hep$^I$ with two phosphate groups (Z$_{2P}$), one phosphate group and one diphosphate group (Z$_{3P}$), or one phosphate and one ethanolamine diphosphate group (Z$_{3PEtn}$), respectively. The major B-fragments from the nonreducing end of the octasaccharides with $m/z$ 1219.49 and 1299.48 (B$_{1P}$ and B$_{2P}$) and the

Rha-lacking heptasaccharides with $m/z$ 1073.41 and 1153.40 had one phosphate or one diphosphate group on Hep$^{II}$, respectively. Taking into account the location of two phosphorylation sites on Hep$^I$ and one phosphorylation site on Hep$^{II}$ (see structures of OS$_{NaOH}$-I and OS$_{NaOH}$-II), it could be inferred that Etn$P$ is located on Hep$^I$, whereas diphosphate groups may occupy either of the Hep residues.

The $^{13}$C-NMR spectrum of OS$_{HOAc}$ (Fig. 4) contained signals for methyl groups of an N-acetyl group at δ 23.3, an alanyl group at δ 19.9 and Rha (C6) at δ 17.9, a methylene group of Kdo$^I$ (C3) at δ 34.0 and ethanolamine (CH$_2$N) at δ 41.0, three nitrogen-bearing carbons (C2 of Ala, GalN and GlcN) at δ 50.3, 51.0 and 56.8, carbonyl groups of the acyl groups and a carboxyl group (C1) of Kdo$^I$ at δ 172–176 and an O-carbamoyl group (NH$_2$CO) at δ 159.4 (compare δ 159.6 for Cm in the core oligosaccharide of *P. aeruginosa* [34]).

The $^1$H-NMR spectrum of OS$_{HOAc}$ showed signals for methyl groups of an N-acetyl group at δ 2.04 (singlet) on GlcN, an N-alanyl group on GalN at δ 1.62 (two overlapping doublets, $J_{2,3}$ ~6 Hz) and H6 of Rha at δ 1.31 (doublet, $J_{5,6}$ 6.5 Hz) as well as the CH$_2$N group of ethanolamine at δ 3.32 (a broad signal) with the ratios of integral intensivities ≈ 1 : 1 : 0.7 : 0.4. These data were in agreement with the relative content of OS$_{NaOH}$-I and OS$_{NaOH}$-II in the alkaline degradation products of the LPS and indicated that Rha is present in ≈ 70% and Kdo$^{III}$ in ≈ 30% of the initial LPS molecules. They also showed that the content of Etn$P$-containing molecules in OS$_{HOAc}$ is ≈ 60% but it cannot be excluded that the Etn$P$ content in the

$$P\text{-}6\rceil \qquad\qquad P\text{-}2\rceil \quad \lceil(4\text{-}P \qquad\qquad\qquad P\text{-}4\rceil$$

β-GlcN$^{III}$-(1→2)-β-Glc$^I$-(1→3)-α-GalN-(1→3)-α-Hep$^{II}$-(1→3)-α-Hep$^I$-(1→5)-α-Kdo$^I$-(2→6)-β-GlcN$^{II}$-(1→6)-α-GlcN$^I$-(1→*P*

α-L-Rha-(1→6)-α-Glc$^{II}$-(1→4)⌟                α-Kdo$^{II}$-(2→4)⌟

OS$_{NaOH}$-I

$$P\text{-}6\rceil \qquad\qquad P\text{-}2\rceil \quad \lceil(4\text{-}P \qquad\qquad\qquad P\text{-}4\rceil$$

β-GlcN$^{III}$-(1→2)-β-Glc$^I$-(1→3)-α-GalN-(1→3)-α-Hep$^{II}$-(1→3)-α-Hep$^I$-(1→5)-α-Kdo$^I$-(2→6)-β-GlcN$^{II}$-(1→6)-α-GlcN$^I$-(1→*P*

α-Kdo$^{III}$-(2→6)-α-Glc$^{II}$-(1→4)⌟         α-Kdo$^{II}$-(2→4)⌟

OS$_{NaOH}$-II

$$\text{L-Ala-2}\rceil \qquad\qquad P\text{-}6\rceil \qquad R\text{--}P\text{-}2\rceil \quad \lceil(4\text{-}P$$

β-GlcNAc-(1→2)-β-Glc$^I$-(1→3)-α-GalN-(1→3)-α-Hep$^{II}$-(1→3)-α-Hep$^I$-(1→5)-Kdo$^I$

α-L-Rha-(1→6)-α-Glc$^{II}$-(1→4)⌟       Cm-7⌟

OS$_{HOAc}$-I   R = H,   OS$_{HOAc}$-II   R = Etn*P*

$$\text{L-Ala-2}\rceil \qquad\qquad P\text{-}6\rceil \qquad R\text{--}P\text{-}2\rceil \quad \lceil(4\text{-}P$$

β-GlcNAc-(1→2)-β-Glc$^I$-(1→3)-α-GalN-(1→3)-α-Hep$^{II}$-(1→3)-α-Hep$^I$-(1→5)-Kdo$^I$

α-Glc$^{II}$-(1→4)⌟       Cm-7⌟

OS$_{HOAc}$-III   R = H,   OS$_{HOAc}$-IV   R = Etn*P*

**Fig. 2. Structures of OS$_{NaOH}$ and OS$_{HOAc}$ obtained by strong alkaline degradation and mild-acid hydrolysis of the LPS, respectively.** In some OS$_{HOAc}$ molecules position 4 of Hep$^I$ or position 6 of Hep$^{II}$ is occupied by a diphosphate group. All monosaccharides are in the pyranose form and have the D-configuration unless stated otherwise. Cm, carbamoyl; Etn, ethanolamine; Hep, L-*glycero*-D-*manno*-heptose; Kdo, 3-deoxy-D-*manno*-oct-2-ulosonic acid; Rha, rhamnose.

intact LPS is higher because this group may be partially lost during mild-acid degradation of the LPS. The major signals for the methylene group (H3) of Kdo$^I$ were observed at δ 1.94 and 2.25. The alanine signal was split owing to the presence of two types of molecules, one containing and the other lacking Rha. The $^{31}$P-NMR spectrum of OS$_{HOAc}$ showed signals for monophosphate and diphosphate groups at δ 1–3 and −10 to −8 (at pD 3), respectively.

The $^1$H-NMR spectrum of the OS$_{HOAc}$ was too complex to be fully assigned by two-dimensional NMR experiments owing to high degree of structural heterogeneity due to the occurrence of two outer core glycoforms, multiple forms of Kdo$^I$ and nonstoichiometric phosphorylation. However, the $^1$H,$^{31}$P HMQC and $^1$H,$^{31}$P HMQC-TOCSY spectra of OS$_{HOAc}$ showed essentially the same correlation pattern as the corresponding spectra of the core oligosaccharides obtained by mild-acid degradation of the *P. aeruginosa* LPS [35,36]. Particularly, the signals of the diphosphate diester group gave correlations to CH$_2$O of ethanolamine and H2 of Hep$^I$ at δ −9.9/4.26 and −9.6/4.63 in the $^1$H,$^{31}$P HMQC spectrum, and, in addition, to CH$_2$N of ethanolamine and H1 of Hep$^I$ at δ −9.9/3.32 and −9.6/5.37 in the $^1$H,$^{31}$P HMQC-TOCSY spectrum, respectively. This finding showed that Etn*PP* group in the LPS of *P. syrinage* is located at the same position as in the *P. aeruginosa* LPS, i.e. at Hep$^I$ O2. The monophosphate groups showed cross-peaks, which could be assigned to correlations to H4 of Hep$^I$ and H6 and Hep$^{II}$, as well as to a minor part of H2 of Hep$^I$ because substitution with Etn*P* is incomplete. Signals

for minor diphosphate monoester groups were too weak and gave no cross-peaks; their location at two other phosphorylation sites, i.e. Hep$^I$ O4 and Hep$^{II}$ O6, could be inferred from the CSD MS data of OS$_{HOAc}$ (see above).

These data defined the structure of the OS$_{HOAc}$ (Fig. 2) as well as of the full core oligosaccharide of *P. syringae* pv. *phaseolicola* GSPB 711 (Fig. 5). The structure of the *P. syringae* LPS core is similar but not identical to that of other members of the genus *Pseudomonas* studied so far, including *P. aeruginosa* [22,30,35–39], *P. fluorescens* [25,29], *P. stutzeri* [40] and *P. tolaasii* [41]. In all these bacteria, the inner core region has the same carbohydrate backbone and may differ only in the presence and the content of diphosphate and ethanolamine diphosphate groups. Therefore, the structure of the inner core may serve as a chemotaxonomic marker for the genus *Pseudomonas*. On the other hand, the outer core region varies in composition and structure in different *Pseudomonas* species, that of *P. syringae* being distinguished by the simultaneous presence of GlcNAc and Rha. The same LPS core composition was revealed by other studies in all *P. syringae* strains tested [11,13–16], and, hence, it may be used as a chemotaxonomic marker for the *P. syringae* group of bacteria, which to date has an uncertain taxonomic status.

A peculiar structural feature of the *P. syringae* LPS studied in this work is the existence of two outer core glycoforms terminated with either Rha or Kdo. A similar alternation of terminal GlcNAc and Kdo residues on a Gal residue has been reported in the outer core region of *Proteus*

**Fig. 3. Capillary skimmer dissociation negative ion ESI FT-ICR mass spectrum of OS$_{HOAc}$ obtained by mild-acid hydrolysis of the LPS and extensions of the regions of the B- and Z-fragment ions due to the cleavage between the Hep residues.** $M_{2P}$, $M_{3P}$, $M_{4P}$ refer to the molecular ions and $Z_{1P}$, $Z_{2P}$, $B_{1P}$, $B_{2P}$ to the fragment ions with one to four phosphate groups. For abbreviations see legend to Fig. 2.



**Fig. 4. $^{13}$C-NMR spectrum of OS$_{HOAc}$ obtained by mild-acid hydrolysis of the LPS.** For abbreviations see legend to Fig. 2.

Glycoform 1

$$
\begin{array}{c}
\text{L-Ala-2}\rceil \qquad\qquad \text{Etn}P\text{- - -}P\text{-2}\rceil \quad \lceil(4\text{-}P \\
\beta\text{-GlcNAc-}(1\rightarrow2)\text{-}\alpha\text{-Glc}^I\text{-}(1\rightarrow3)\text{-}\alpha\text{-GalN-}(1\rightarrow3)\text{-}\alpha\text{-Hep}^{II}\text{-}(1\rightarrow3)\text{-}\alpha\text{-Hep}^I\text{-}(1\rightarrow5)\text{-Kdo}^I\text{-}(2\rightarrow \\
\alpha\text{-L-Rha-}(1\rightarrow6)\text{-}\beta\text{-Glc}^{II}\text{-}(1\rightarrow4)\rfloor \qquad \text{Cm-7}\rfloor \ \lfloor(6\text{-}P \qquad \alpha\text{-Kdo}^{II}\text{-}(2\rightarrow4)\rfloor
\end{array}
$$

Glycoform 2

$$
\begin{array}{c}
\text{L-Ala-2}\rceil \qquad\qquad \text{Etn}P\text{- - -}P\text{-2}\rceil \quad \lceil(4\text{-}P \\
\beta\text{-GlcNAc-}(1\rightarrow2)\text{-}\alpha\text{-Glc}^I\text{-}(1\rightarrow3)\text{-}\alpha\text{-GalN-}(1\rightarrow3)\text{-}\alpha\text{-Hep}^{II}\text{-}(1\rightarrow3)\text{-}\alpha\text{-Hep}^I\text{-}(1\rightarrow5)\text{-Kdo}^I\text{-}(2\rightarrow \\
\alpha\text{-Kdo}^{III}\text{-}(2\rightarrow6)\text{-}\beta\text{-Glc}^{II}\text{-}(1\rightarrow4)\rfloor \qquad \text{Cm-7}\rfloor \ \lfloor(6\text{-}P \qquad \alpha\text{-Kdo}^{II}\text{-}(2\rightarrow4)\rfloor
\end{array}
$$
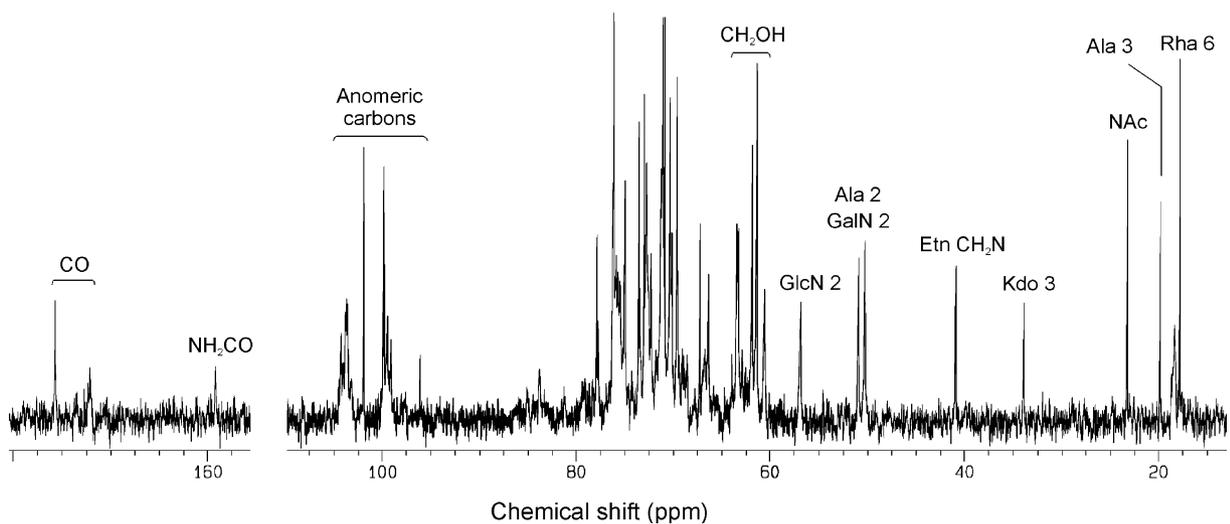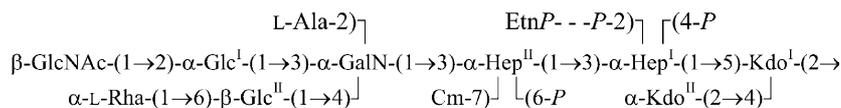
**Fig. 5. Structures of the core region of the *P. syringae* LPS.** In some molecules, position 4 of Hep$^I$ or position 6 of Hep$^{II}$ is occupied by a diphosphate group. Dashed line indicates a nonstoichiometric substitution. For abbreviations see legend to Fig. 2.

*vulgaris* O25 [42]. Two isomeric outer core glycoforms differing in the postion of a terminal Rha residue occurs in the *P. aeruginosa* LPS [30], one of them being markedly similar to the Rha-containing glycoform of the *P. syringae* LPS core. This glycoform and only this glycoform serves to accept the O-polysaccharide chain in *P. aeruginosa* LPS [22,36–39], and its *P. syringae* counterpart can be assumed to have the same function. A presumable biological role of this phenomenon in smooth strains is a regulation of the content of LPS molecules with short and long carbohydrate chains on the cell surface by a predominant production of the appropriate core glycoform.

It should be noted that studies with LPS-specific monoclonal antibodies aiming at development of a recognition tool for *P. syringae* strains revealed two types of the LPS core in various strains of *P. syringae* [17,18]. The structure of one of them, which is shared by most strains tested [17,18], was established in this work, whereas the other structure remains to be determined. Taking into account that monoclonal antibodies recognize usually the most peripheral LPS structures distal from lipid A, it can be supposed that the structural difference(s) between the two serological core types is located in the outer core region. Further studies are necessary to find out if the two core types in various strains are related to the two core glycoforms revealed in *P. syringae* pv. *phaseolicola* GSPB 711.

## Acknowledgements

## References

1. Young, J.M., Saddler, G.S., Takikawa, Y., DeBoer, S.H., Vauterin, L., Gardan, L., Gvozdyak, R.I. & Stead, D.E. (1996) Names of plant pathogenic bacteria 1864–1995. ISPP Subcommittee on Taxonomy of Plant Pathogenic Bacteria. *Rev. Plant Pathol.* **75**, 721–763.

2. Gardan, L., Shafik, H., Belouin, S., Broch, R., Grimont, F. & Grimont, P.A. (1999) DNA relatedness among the pathovars of *Pseudomonas syringae* and description of *Pseudomonas tremae* sp. nov. & *Pseudomonas cannabina* sp. nov. (ex Sutic and Dowson 1959). *Int. J. Syst. Bacteriol.* **49**, 469–478.

3. Knirel, Y.A. & Kochetkov, N.K. (1994) The structure of lipopolysaccharides of gram-negative bacteria. III. The structure of O-antigens. *Biochemistry (Mosc.)* **59**, 1325–1383.

4. Ovod, V., Zdorovenko, E.L., Shashkov, A.S., Kocharova, N.A. & Knirel, Y.A. (2000) Structure of the O polysaccharide and serological classification of *Pseudomonas syringae* pv. *ribicola* NCPPB 1010. *Eur. J. Biochem.* **267**, 2372–2379.

5. Zdorovenko, E.L., Knirel, Y.A. & Ovod, V.V. (1999) Structures of O-polysaccharide chains of *Pseudomonas syringae* pv. *garcae* LPS. Abstract. 13th International Congress Hungarian Soc. Microbiol. Budapest, 29 August–1 September 1999, Hungarian Soc. Microbiol, p. 112.

6. Zdorovenko, E.L., Ovod, V., Shashkov, A.S., Kocharova, N.A., Knirel, Y.A. & Krohn, K. (1999) Structure of the O-polysaccharide of the lipopolysaccharide of *Pseudomonas syringae* pv. *garcae* ICMP 8047. *Biochemistry (Mosc.)* **64**, 765–773.

7. Zdorovenko, E.L., Zatonsky, G.V., Zdorovenko, G.M., Pasichnik, L.A., Shashkov, A.S. & Knirel, Y.A. (2001) Structural heterogeneity in the lipopolysaccharides of *Pseudomonas syringae* with O-polysaccharide chains having different repeating units. *Carbohydr. Res.* **336**, 329–336.

8. Zdorovenko, E.L., Zatonsky, G.V., Kocharova, N.A., Shashkov, A.S., Knirel, Y.A. & Ovod, V. (2002) Structure of the O-polysaccharide of *Pseudomonas syringae* pv. *delphinii* NCPPB 1879$^T$ having side chains of 3-acetamido-3,6-dideoxy-D-galactose residues. *Biochemistry (Mosc.)* **67**, 558–565.

9. Zdorovenko, E.L., Zatonsky, G.V., Kocharova, N.A., Shashkov, A.S., Knirel, Y.A. & Ovod, V. (2003) Structures of the O-polysaccharides of two strains of *Pseudomonas syringae* pv. *porri* from genomospecies 4. *Eur. J. Biochem.* **270**, 20–27.

10. Ovod, V., Zdorovenko, E.L., Shashkov, A.S., Kocharova, N.A. & Knirel, Y.A. (2004) Structural diversity of the O polysaccharides of the lipopolysaccharides of *Pseudomonas syringae* pv. *garcae* and other strains from genomospecies 4. *Mikrobiologiya* **73**, 777–789.

11. Zdorovenko, G.M., Shashkov, A.S., Zdorovenko, E.L., Kocharova, N.A., Yakovleva, L.M., Knirel, Y.A. & Rudolph, K. (2001) Characterization of the lipopolysaccharide and structure of the O-specific polysaccharide of the bacterium *Pseudomonas syringae* pv. *atrofaciens* IMV 948. *Biochemistry (Mosc.)* **66**, 369–377.

12. Knirel, Y.A. & Zdorovenko, G.M. (1997) Structures of O-polysaccharide chains of lipopolysaccharides as the basis for classification of *Pseudomonas syringae* and related strains. In *Proceedings of the 5th Intern. Working Group on Pseudomonas Syringae Pathovars and Related Pathogens*. Berlin, September 3–8, 1995

(Rudolph, K., Burr, T.J., Mansfield, J.W., Stead, D., Vivian, A. & von Kietzell, J., eds), pp. 475–480. Kluwer Academic Publishers, Dordrecht, Boston, London.

13. Zdorovenko, G.M., Gubanova, N.Y., Solyanik, L.P., Knirel, Y.A., Yakovleva, L.M. & Zakarova, I.Y. (1991) Composition and structure of lipopolysaccharides from the strains of different pathovars of *Pseudomonas syringae*. *Proceedings of the 4th International Working Group on Pseudomonas Syringae Pathovars*, ISPP Committee on Phytopathogenic Bacteria and Università di Firenze. Florence, 1991, pp. 391–401.

14. Zdorovenko, G.M., Solyanic, L.P., Yakovleva, L.M. & Paramonov, N.A. (1997) Characterization of O-antigens from different strains of *Pseudomonas syringae* pv. *tabaci*. *Biochem. (Mosc.)* **62**, 28–37.

15. Zdorovenko, G.M., Varbanets, L.D., Zdorovenko, E.L., Vinarskaya, N.V. & Yakovleva, L.M. (2004) Chemical-biological characterization of the lipopolysaccharides from collection culture of *Pseudomonas syrnigae* pv. *maculicola* IMV 381 and its dissociants. *Mikrobiologiya* **73**, 1–12.

16. Gross, M., Mayer, H., Widemann, C. & Rudolph, K. (1988) Comparative analysis of the lipopolysaccharides of a rough and a smooth strain of *Pseudomonas syringae* pv. *phaseolicola*. *Arch. Microbiol.* **149**, 372–376.

17. Ovod, V., Rudolph, K. & Krohn, K. (1997) Serological classification of *Pseudomonas syringae* pathovars based on monoclonal antibodies towards the lipopolysaccharide O-chains. In *Proceedings of the 5th Intern. Working Group on Pseudomonas Syringae Pathovars and Related Pathogens*. Berlin, September 3–8, 1995 (Rudolph, K., Burr, T.J., Mansfield, J.W., Stead, D., Vivian, A. & von Kietzell, J., eds), pp. 526–531. Kluwer Academic Publishers, Dordrecht, Boston, London.

18. Ovod, V., Rudolph, K., Knirel, Y.A. & Krohn, K. (1996) Immunochemical characterization of O polysaccharides composing the α-D-rhamnose backbone of lipopolysaccharide of *Pseudomonas syringae* and classification of bacteria into serogroups O1 and O2 with monoclonal antibodies. *J. Bacteriol.* **178**, 6459–6465.

19. Galanos, C., Lüderitz, O. & Westphal, O. (1969) A new method for the extraction of R lipopolysaccharides. *Eur. J. Biochem.* **9**, 245–249.

20. Ciucanu, I. & Kerek, F. (1984) A simple and rapid method for the permethylation of carbohydrates. *Carbohydr. Res.* **131**, 209–217.

21. Holst, O. (2000) Deacylation of lipopolysaccharides and isolation of oligosaccharide phosphates. In *Bacterial Toxins. Methods and Protocols* (Holst, O., ed.), pp. 345–353. Humana Press, Totowa, New Jersey.

22. Bystrova, O.V., Shashkov, A.S., Kocharova, N.A., Knirel, Y.A., Lindner, B., Zähringer, U. & Pier, G.B. (2002) Structural studies on the core and the O-polysaccharide repeating unit of *Pseudomonas aeruginosa* immunotype 1 lipopolysaccharide. *Eur. J. Biochem.* **269**, 2194–2203.

23. Bystrova, O.V., Shashkov, A.S., Kocharova, N.A., Knirel, Y.A., Zähringer, U. & Pier, G.B. (2003) Elucidation of the structure of the lipopolysaccharide core and the linkage between the core and the O-antigen in *Pseudomonas aeruginosa* immunotype 5 using strong alkaline degradation of the lipopolysaccharide. *Biochemistry (Mosc.)* **68**, 918–925.

24. Lipkind, G.M., Shashkov, A.S., Knirel, Y.A., Vinogradov, E.V. & Kochetkov, N.K. (1988) A computer-assisted structural analysis of regular polysaccharides on the basis of ¹³C-NMR data. *Carbohydr. Res.* **175**, 59–75.

25. Knirel, Y.A., Grosskurth, H., Helbig, J.H. & Zähringer, U. (1995) Structures of decasaccharide and tridecasaccharide tetraphosphates isolated by strong alkaline degradation of O-deacylated lipopolysaccharide of *Pseudomonas fluorescens* strain ATCC 49271. *Carbohydr. Res.* **279**, 215–226.

26. Bock, K. & Pedersen, C. (1983) Carbon-13 nuclear magnetic resonance spectroscopy of monosaccharides. *Adv. Carbohydr. Chem. Biochem.* **41**, 27–66.

27. Kosma, P., D'Souza, F.W. & Brade, H. (1995) Synthesis of Kdo-trisaccharide derivatives of chlamydial and enterobacterial LPS containing carboxyl-reduced or β-configurated Kdo-residues. *J. Endotoxin Res.* **2**, 63–76.

28. Jansson, P.-E., Kenne, L. & Widmalm, G. (1989) Computer-assisted structural analysis of polysaccharides with an extended version of CASPER using ¹H- and ¹³C-N.M.R. data. *Carbohydr. Res.* **188**, 169–191.

29. Knirel, Y.A., Helbig, J.H. & Zähringer, U. (1996) Structure of a decasaccharide isolated by mild acid degradation and dephosphorylation of the lipopolysaccharide of *Pseudomonas fluorescens* strain ATCC 49271. *Carbohydr. Res.* **283**, 129–139.

30. Knirel, Y.A., Bystrova, O.V., Shashkov, A.S., Kocharova, N.A., Senchenkova, S.N., Moll, H., Lindner, B., Zähringer, U., Hatano, K. & Pier, G.B. (2001) Structural analysis of the lipopolysaccharide core of a rough, cystic fibrosis isolate of *Pseudomonas aeruginosa*. *Eur. J. Biochem.* **268**, 4708–4719.

31. Sadovskaya, I., Brisson, J.-R., Lam, J.S., Richards, J.C. & Altman, E. (1998) Structural elucidation of the lipopolysaccharide core regions of the wild-type strain PAO1 and O-chain-deficient mutant strains AK1401 and AK1012 from *Pseudomonas aeruginosa* serotype O5. *Eur. J. Biochem.* **255**, 673–684.

32. Beckmann, F., Moll, H., Jäger, K.-E. & Zähringer, U. (1995) 7-O-Carbamoyl-L-*glycero*-D-*manno*-heptose: a new core constituent in the lipopolysaccharide of *Pseudomonas aeruginosa*. *Carbohydr. Res.* **267**, C3–C7.

33. Olsthoorn, M.M.A., Haverkamp, J. & Thomas-Oates, J.E. (1999) Mass spectrometric analysis of *Klebsiella pneumoniae* ssp. *pneumoniae* rough strain R20 (O1⁻:K20⁻) lipopolysaccharide preparations: Identification of novel core oligosaccharide components and three 3-deoxy-D-*manno*-oct-2-ulopyranosonic artifacts. *J. Mass Spectrom.* **34**, 622–636.

34. Sanchez-Carballo, P.M., Rietschel, E.T., Kosma, P. & Zähringer, U. (1999) Elucidation of the structure of an alanine-lacking core tetrasaccharide trisphosphate from the lipopolysaccharide of *Pseudomonas aeruginosa* mutant H4. *Eur. J. Biochem.* **261**, 500–508.

35. Kooistra, O., Bedoux, G., Brecker, L., Lindner, B., Sanchez-Carballo, P., Haras, D. & Zähringer, U. (2003) Structure of a highly phosphorylated lipopolysaccharide core in the *algC* mutants derived from *Pseudomonas aeruginosa* wild-type strains PAO1 (serogroup O5) and PAC1R (serogroup O3). *Carbohydr. Res.* **338**, 2667–2677.

36. Bystrova, O.V., Lindner, B., Moll, H., Kocharova, N.A., Knirel, Y.A., Zähringer, U. & Pier, G.B. (2003) Structure of the lipopolysaccharide of *Pseudomonas aeruginosa* O-12 with a randomly O-acetylated core region. *Carbohydr. Res.* **338**, 1895–1905.

37. Bystrova, O.V., Lindner, B., Moll, H., Kocharova, N.A., Knirel, Y.A., Zähringer, U. & Pier, G.B. (2003) Structure of the biological repeating unit of the O-antigen of *Pseudomonas aeruginosa* immunotype 4 containing both 2-acetamido-2,6-dideoxy-D-glucose and 2-acetamido-2,6-dideoxy-D-galactose. *Carbohydr. Res.* **338**, 1801–1806.

38. Bystrova, O.V., Lindner, B., Moll, H., Kocharova, N.A., Shashkov, A.S., Knirel, Y.A., Zähringer, U. & Pier, G.B. (2004) Full structure of the lipopolysaccharide of *Pseudomonas aeruginosa* immunotype 5. *Biochemistry (Mosc.)* **69**, 170–175.

39. Sadovskaya, I., Brisson, J.-R., Thibault, P., Richards, J.C., Lam, J.S. & Altman, E. (2000) Structural characterization of the outer core and the O-chain linkage region of lipopolysaccharide from *Pseudomonas aeruginosa* serotype O5. *Eur. J. Biochem.* **267**, 1640–1650.

40. Leone, S., Izzo, V., Silipo, A., Sturiale, L., Garozzo, D., Lanzetta, R., Parrilli, M., Molinaro, A. & Di Donato, A. (2004) A novel type of highly negatively charged lipooligosaccharide from *Pseudomonas stutzeri* OX1 possessing two 4,6-*O*-(1-carboxy)-ethylidene residues in the outer core region. *Eur. J. Biochem.* **271**, 2691–2704.

41. Silipo, A., Leone, S., Molinaro, A., Lanzetta, R. & Parrilli, M. (2004) The structure of the phosphorylated carbohydrate backbone of the lipopolysaccharide of the phytopathogen bacterium *Pseudomonas tolaasii. Carbohydr. Res.* **339**, 2241–2248.

42. Vinogradov, E., Cedzynski, M., Rozalski, A., Ziolkowski, A. & Swierzko, A. (2000) The structure of the carbohydrate backbone of the core–lipid A region of the lipopolysaccharide from *Proteus vulgaris* serotype O25. *Carbohydr. Res.* **328**, 533–538.